Hindawi
Mobile Information Systems
Volume 2022, Article ID 1335829, 8 pages
https://doi.org/10.1155/2022/1335829

Research Article

On Element Selection in STAR-RIS for NOMA Transmission

Bin Sheng [1,2]

[1]*National Mobile Communications Research Laboratory, Southeast University, Nanjing 210096, China*
[2]*Purple Mountain Laboratories, Nanjing 211100, China*

Correspondence should be addressed to Bin Sheng; sbdtt@seu.edu.cn

Received 2 November 2021; Revised 17 January 2022; Accepted 12 February 2022; Published 8 March 2022

Academic Editor: Adrian Kliks

Reconfigurable intelligent surface (RIS) is a promising solution to build a programmable wireless propagation environment through reflecting the incident signals with a large number of low-cost passive elements. Recently, a novel concept of simultaneous transmitting and reflecting RIS (STAR-RIS) has been proposed, where incident signals can be transmitted and reflected to users located on different sides of the surface. Therefore, there are two coefficients that needed to be configured for each element of STAR-RIS. One is used to adjust the phase shifts and amplitudes of the transmitted signal; the other is configured for the reflected signal. In some harsh situations where the direct links between access points (AP) and users are blocked, STAR-RIS can be deployed to provide additional signal propagation paths. With the aid of STAR-RIS, multiple users can share the same time-frequency resources and transmit signals in a power-domain nonorthogonal multiple access (NOMA) case. However, when the users move into cell edge where they have almost the same transmit power and distance to AP, the system performance will degrade largely. To solve this problem, a novel element selection method is proposed, which can reshape the channel to a favorable propagation environment, for NOMA by only activating the appropriate elements in STAR-RIS.

1. Introduction

The rapid development of the mobile Internet and the Internet of Things (IoT) exponentially accelerates the demand for high system capacity and low transmission latency in future wireless communications. Nonorthogonal multiple access (NOMA) has been recently recognized as an effective multiple access technique for its capability of providing a significantly improved spectral efficiency (SE), by multiplexing multiple users in the same resource (e.g., time, frequency, and code) block. Specifically, power-domain NOMA assigns different powers to different users, which have distinct channel gains at the transmitter and decodes their data flows at the receiver by using a successive-interference-cancellation (SIC) technique [1]. Consequently, this technique is pretty suitable for use in massive wireless connectivity scenarios, since there are usually not enough resources for such a huge number of users to transmit data sequences simultaneously. Moreover, superimposition of users' signals can reduce communication latency significantly, which is another requirement of the massive wireless connectivity scenario [2, 3]. However, it should be noted that NOMA does not always outperform traditional orthogonal multiple access (OMA). For instance, in a downlink multiple-input-single-output (MISO) system, when the users have mutually orthogonal channels, traditional spatial division multiple access (SDMA) can achieve better performance. The other drawback of NOMA is that under the consideration of user fairness, the performances of strong users are affected heavily by the power allocation to the users with weak channel conditions [4].

Through using various new technologies such as ultra-dense network (UDN), massive multiple-input multiple-output (MIMO), and millimeter-wave (mmWave) communication, the fifth-generation (5G) wireless network can achieve an almost 1000-fold network capacity increase and ubiquitous wireless connectivity for at least 100 billion devices [5]. However, the densely deployed base stations (BSs), each with a large number of antennas, require inevitably more complex signal processing as well as costlier and energy-consuming hardware (e.g., radio frequency (RF) chains). Moreover, due to the high path loss, the line-of-

sight (LOS) channel between the transceivers is often needed in mmWave communication. However, it is often unavailable due to frequent blockages [6]. Recently, as a potential technology to solve all these problems, reconfigurable intelligent surfaces (RIS) have drawn a great deal of attention. RIS is a planar surface comprising a large number of low-cost passive reflecting and programmable elements [7, 8]. It can be implemented based on the concept of "metasurface," which is made of massive so-called meta-atoms with an electrical thickness in the order of the sub-wavelength of the operating frequency of interest. As shown in Figure 1, a typical architecture of RIS consists of three layers and a smart controller. The outer layer is made of a dielectric substrate with a large number of metallic patches (elements) printed on it. This layer is designed to directly interact with incident signals. To avoid signal energy leakage, a copper plate is embedded behind the outer layer. In the inner layer, a control circuit board is used to adjust the reflection amplitude and phase shift of each element on the outer layer. It is controlled by a smart controller, which also acts as a gateway to communicate and coordinate with other network components, such as BSs and user terminals, through separate wired or wireless links. Although RISs can be seen as a broadband technology, under some scenarios where a system is working in a particular frequency band, specific element designs are required. In microwave frequency bands, PIN diodes are mainly used in current designs. Flexible materials such as liquid crystal and graphene are considered for millimeter-wave and terahertz bands. Let us take a PIN diode, for example. By controlling its biasing voltage via a direct-current (DC) feeding line, it can be switched between the states of "On" and "Off" with their equivalent circuits shown in Figure 1. In this case, the two states generate a phase-shift difference of π in rad for incident signals. On the other hand, the reflection amplitude can be controlled by embedding a variable resistor load in each element. By changing the values of resistors, different portions of the incident signal's energy are absorbed, which makes the reflection amplitude vary in [0, 1]. By properly designing these elements, such as geometrical shape, orientation, arrangement, and so on, they can reflect the incident signals with different amplitudes and phase shifts. The reflected signals are thereby combined to collaboratively reconfigure the propagation channel to achieve certain communication objectives such as interference mitigation and received-signal power-boosting [9, 10].

Based on the provided additional links, RISs can be used to enrich the channel scattering environment, increase multiplexing gain, enhance coverage in dead zones, and so on. Furthermore, it provides new dynamic configuration solutions for new applications such as communication network security and simultaneous wireless information and power transmission (SWIPT) [11]. However, towards the road of practical application, RISs face many technical and engineering challenges that need to be solved. The introduction of RISs destroys the reciprocity of the uplink and downlink in most cases, and for RISs with discrete phases used in practice, the nonreciprocal characteristics will face more severe design difficulties. Additionally, the dense

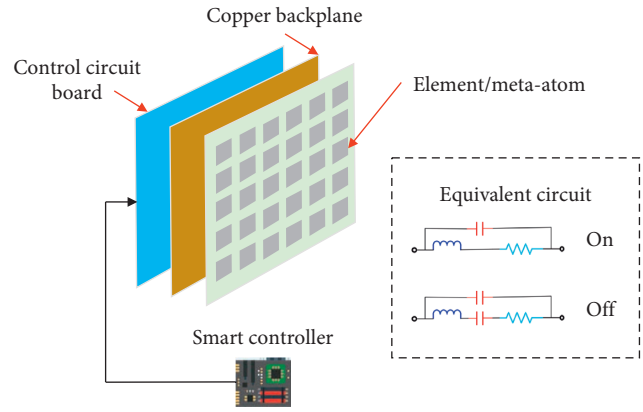

Figure 1: Architecture of RIS.

arrangement of massive elements in a broad area makes it difficult to model the near-field propagation and analyze the channel correlations. Furthermore, the huge number of elements makes channel estimation difficult to perform and will waste lots of pilot resources or training time [12].

RIS can be explored to enhance the performance of NOMA by providing additional channel paths. These channel paths are intelligently reconfigured to overcome the drawbacks of the NOMA technique (e.g., the users' channels are close to mutually orthogonal). By adjusting the RIS's phase shifts, RIS-assisted NOMA systems can achieve better performance under the user fairness guarantee. Moreover, compared with the current relaying technique, RISs can work in a nearly passive mode which reduces energy consumption and hardware costs. Driven by these advantages, the combination of NOMA with RISs has drawn considerable attention in a few recent works. In [13], a simple design of RIS-aided NOMA has been proposed, which can accommodate more users on each orthogonal spatial direction than that of SDMA. The potential gains of adopting RISs, in terms of energy efficiency, sum-rate, and outage performance have been demonstrated in [14]. By jointly optimizing the BS's transmission beamforming and the RIS's phase shifts, the total transmit power can be minimized with a maximized sum rate [15]. Recently, a novel concept of simultaneous transmitting and reflecting RIS (STAR-RIS) has been proposed, where incident signals can be transmitted and reflected to users located on different sides of the surface [16]. Its prototype has been developed by NTT DoCoMo, which verified the practical impenetrability of STAR-RIS [17]. Different from conventional RISs, there are two coefficients needed to be configured for each element of STAR-RIS. One is used to adjust the phase shifts and amplitudes of the transmitted signal; the other is configured for the reflected signal. By jointly optimizing the transmission and reflection coefficients, the coverage of STAR-RIS aided NOMA can be largely extended when compared with conventional reflecting and transmitting only RIS [18].

In STAR-RIS aided power-domain NOMA, multiple users can transmit signals to an access point (AP) on the same time-frequency resources but with different power levels. However, in some cases, when the users move into

the cell edge, they may have to transmit the signal using the same maximum power. Furthermore, in this area, the users usually have an equal distance to STAR-RIS, which makes their signals undergo the same large-scale fading due to the dominant LOS paths. At AP, since the arriving signal has almost the same power, it is hard to perform successive interference cancelation properly, which results in a large degradation of performance. Therefore, how to improve the performance of cell edge users has become a crucial issue to be tackled for cellular systems. Unfortunately, there are no existing NOMA-related literature concerning this issue and thereby no method can be found to solve this problem. Although traditional OMA systems can exploit coordinated multiple points (CoMP) transmission techniques to improve cell edge performance, more consumption of resources and energy is inevitable. To solve this problem, we propose a novel STAR-RIS aided NOMA method in this paper. The main contribution of this method is that, through selecting the appropriate elements in STAR-RIS to activate, the channels between users and AP are reshaped into a new propagation situation where the signals arrive at AP with different powers level. Since this is a favorable wireless environment for NOMA transmission, superior performance is then obtained, when compared with the conventional method where all the elements are active.

The rest of this paper is organized as follows. The system model and problem formulation are presented in Section II. A novel method is proposed to solve the problem in Section III. Section IV presents the numerical results. Section V concludes this paper.

2. System Model

We consider a narrow-band uplink NOMA system operating over frequency-flat channels, where several single-antenna users communicate with a single-antenna AP. Assume the direct links between AP and users are blocked by obstacles, and a STAR-RIS consisting of M elements is then employed to create a virtual propagation path between them. In practice, the STAR-RIS is usually deployed in a way that it is not only in LOS with the AP, but also close to the users. So, we further assume that all the channels are dominated by LOS paths. Notice that, for NOMA transmission, if too many users are served, the effective performance gain will saturate quickly with a rapidly growing receiver complexity [14]. Thus, two users, labeled by A and B, are considered in this paper which transmit signals on the same time-frequency resources, but with different power levels. Furthermore, we assume that user A is located behind the STAR-RIS, while user B stays in front of the STAR-RIS. In this case, their signals can be transmitted and reflected to AP simultaneously. Usually, the STAR-RIS is controlled by AP through a wireless or fiber link and the reflection and transmission coefficients of each element can therefore be adjusted by AP, as shown in Figure 2.

Assuming the channel between STAR-RIS and user k, $k \in \{A, B\}$, follows Rician fading distribution, we obtain

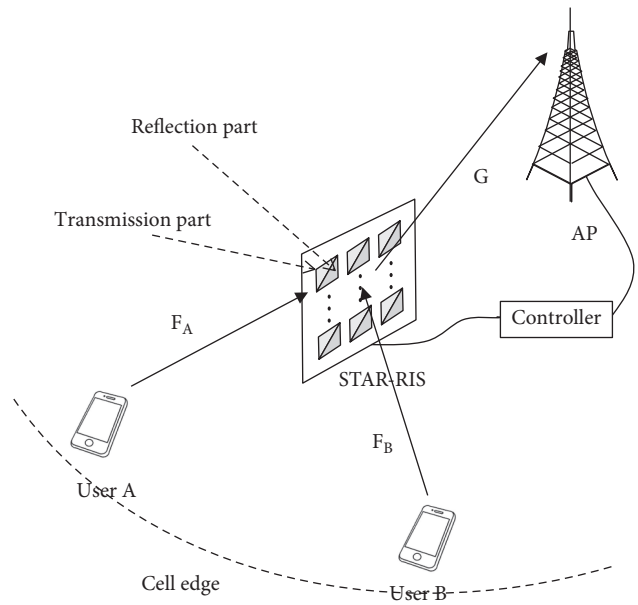

Figure 2: An illustration of STAR-RIS aided NOMA for cell-edge users.

$$F_k = \sqrt{\frac{\rho_0}{d_k^{\alpha_{\mathrm{RU}}}}}\left(\sqrt{\frac{K_1}{K_1+1}}f_k^{\mathrm{LOS}} + \sqrt{\frac{1}{K_1+1}}f_k^{\mathrm{NLOS}}\right), \tag{1}$$

where $d_{k.}$ denotes the distance between STAR-RIS and user k, $\alpha_{\mathrm{RU.}}$ represents the path loss exponent, K_1. denotes the Rician factor, and ρ_0. is the path loss at a reference distance of one meter. f_k^{LOS}. and f_k^{NLOS}. are both M by one vector with their elements denoting the deterministic LOS components and the random nonline-of-sight (NLOS) components, respectively, of the channels from user k to each element in STAR-RIS. Moreover, each entry in f_k^{NLOS}. is modeled as an independent and identically distributed Rayleigh random variable. Similarly, the channel between STAR-RIS and AP can be written by

$$G = \sqrt{\frac{\rho_0}{d_0^{\alpha_{\mathrm{AR}}}}}\left(\sqrt{\frac{K_2}{K_2+1}}g^{\mathrm{LOS}} + \sqrt{\frac{1}{K_2+1}}g^{\mathrm{NLOS}}\right), \tag{2}$$

where d_0. is the distance between STAR-RIS and AP, α_{AR}. is path loss exponent, and K_2. denotes the Rician factor of the RIS-to-AP channel. g^{Los}. and g^{NLOS}. are the LOS and NLOS components, respectively. Finally, the cascade channels for users A and B can be expressed by

$$h_k = G^H O_k F_k, k \in \{\mathrm{A}, \mathrm{B}\}, \tag{3}$$

where $O_{\mathrm{A}} = \sqrt{\beta_{\mathrm{A}}}\mathrm{diag}(e^{j\theta_0^{\mathrm{A}}}, e^{j\theta_1^{\mathrm{A}}}, \ldots, e^{j\theta_{M-1}^{\mathrm{A}}})$ and $O_{\mathrm{B}} = \sqrt{\beta_{\mathrm{B}}}\mathrm{diag}(e^{j\theta_0^{\mathrm{B}}}, e^{j\theta_1^{\mathrm{B}}}, \ldots, e^{j\theta_{M-1}^{\mathrm{B}}})$, denote the transmission and reflection coefficient matrices, respectively. Here, $\sqrt{\beta_{\mathrm{A}}}$, $\sqrt{\beta_{\mathrm{B}}} \in [0,1]$, and θ_m^A, $\theta_m^{\mathrm{B}} \in [0, 2\pi)$, characterize the amplitude and phase shift adjustments imposed on the incident signals facilitated by the m-th element during transmission and reflection, respectively. To reduce the signaling overhead between the STAR-RIS and its controlling AP, all elements are assumed to have the same

adjusting amplitude coefficients and $\beta_A + \beta_B = 1$ for the sake of energy conservation [19].

Under the assumption that the synchronization is perfect and the channel is constant during the period of NOMA transmission, the baseband equivalent discrete-time signal at AP can be written as

$$y(n) = \sqrt{P_A}x_A(n)h_A + \sqrt{P_B}x_B(n)h_B + w(n), \quad (4)$$

where $x_A(n)$ and $x_B(n)$ denote the data symbols transmitted by users A and B, at the n-th time instant. They belong to a finite-alphabet complex constellation with unit energy. P_A, and P_B, represent the transmit power of users A and B, respectively. $w(n)$, is the additive white complex Gaussian noise (AWGN) with zero mean and variance $E\{|w(n)|^2\} = \sigma_n^2$,. According to the principle of NOMA, for the case of $|h_A|^2 > |h_B|^2$, we should set $P_A < P_B$, to facilitate SIC at receiver. SIC is a well-known physical layer technique which has the ability to receive two or more signals concurrently without causing a collision. The basic principle is that the receiver first decodes the strong signal, and then subtracts it from the combined signal to extract the weak one from the residue. When decoding the strong signal, the interference introduced by the weak signal can be treated as noise due to its low power. Consequently, if the powers of different signals are similar, the weak signal will generate so much interference that the strong signal cannot be decoded correctly any more. When they have equal power, there is no strong signal and SCI stops working.

In practical systems, when users move into the area of the cell edge, they may have to transmit signals using the same maximum power. Moreover, in this area, the users usually have approximately equal distance to STAR-RIS, which makes their signals arrive at AP with almost the same power. In this case, the SIC is nearly unable to work. To the best of my knowledge, in most NOMA-related research, two types of users, namely near users and cell-edge users, are usually assumed and there are no studies concerning the issue of two cell-edge users, which we will deal with in this paper. So, no existing method can be found to solve this problem.

3. Proposed Method

In order to make SIC work properly, the received powers of users A and B should have different levels, which motivates us to propose an element selection method here. The basic idea of the proposed method can be described as follows. In the concerned STAR-RIS-aided communication system, the signal is transmitted from UE. After being reflected or transmitted by one element in STAR-RIS, it arrives at AP. The channel it experiences can be seen as one individual path. Since the STAR-RIS has M elements, there are M paths from each user to the AP that have different amplitudes and phases. The M paths are finally added together to compose the cascade channel. From all the paths of user A and user B, we can find that some of the paths for user A have greater power than those of user B, while the others are not. So, if we only select the elements that generate the paths with higher power for user A, to active, the signal from user A will experience a stronger channel than that of user B's signal. It should be noted that the phase differences between each selected path can be compensated by adjusting the reflection and transmission coefficients of their related elements. So, they can be combined coherently. Assuming the real channel parameters are available, we can calculate the power of an individual path transmitted or reflected by each element of STAR-RIS for users A and B, as

$$\mu_k(m) = |F_k(m)|^2|G(m)|^2, \quad m = 0, 1, \ldots, M-1, \quad (5)$$

where $F_k(m)$ and $G(m)$ denote the m-th entry of vector F_k and G, respectively. Then, we choose all the elements that satisfy

$$\mu_A(m) > \mu_B(m). \quad (6)$$

To activate and inactivate the rest of the elements during the data transmission period, moreover, in order to maximize the channel gains for both users A and B, we set $\beta_A = \beta_B = 0.5$. On the other hand, all the paths should be combined coherently, otherwise, their random phases will make the channel gain decrease largely. Fortunately, this can be realized by setting the phase shifts of the m-th element to

$$\begin{aligned} \theta_m^A &= -\angle\left(F_A(m) \cdot G(m)\right), \\ \theta_m^B &= -\angle\left(F_B(m) \cdot G(m)\right), \end{aligned} \quad (7)$$

where $\angle(\cdot)$ represents the phase extraction operator.

At AP, since the channel for user A is stronger than that of user B, we first decode user A's signal. By neglecting the interference introduced by user B, we obtain

$$\widehat{x}_A(n) = \frac{y(n)}{\sqrt{P_A}h_A}, \quad (8)$$

where $\widehat{x}_A(n)$ is the estimate of $x_A(n)$. After subtracting user A's signal, we obtain

$$z(n) = y(n) - \sqrt{P_A}\widetilde{x}_A(n)h_A, \quad (9)$$

where $\widetilde{x}_A$ denotes the data symbol reconstructed from $\widehat{x}_A(n)$. Assuming channel coding is not considered, a hard decision is therefore used. We denote the real part and imaginary part of $\widehat{x}_A(n)$, by $\mathrm{Re}\{\widehat{x}_A(n)\}$, and $\mathrm{Im}\{\widehat{x}_A(n)\}$, respectively. We assume QPSK modulation without grey mapping is used at the transmitter and a sign function is defined as follows:

$$\mathrm{sign}(x) = \begin{cases} 1, & x \geq 0, \\ -1, & x < 0. \end{cases} \quad (10)$$

In order to reconstruct a modulated symbol from $\widehat{x}_A(n)$, its real and imaginary parts are first put through a sign function and then added together as

$$\widetilde{x}_A(n) = \frac{1}{\sqrt{2}}\left[\mathrm{sign}\left(\mathrm{Re}\{\widehat{x}_A(n)\}\right) + j \cdot \mathrm{sign}\left(\mathrm{Im}\{\widehat{x}_A(n)\}\right)\right], \quad (11)$$

where j denotes the imaginary unit. Finally, the data symbol of user B can be estimated by

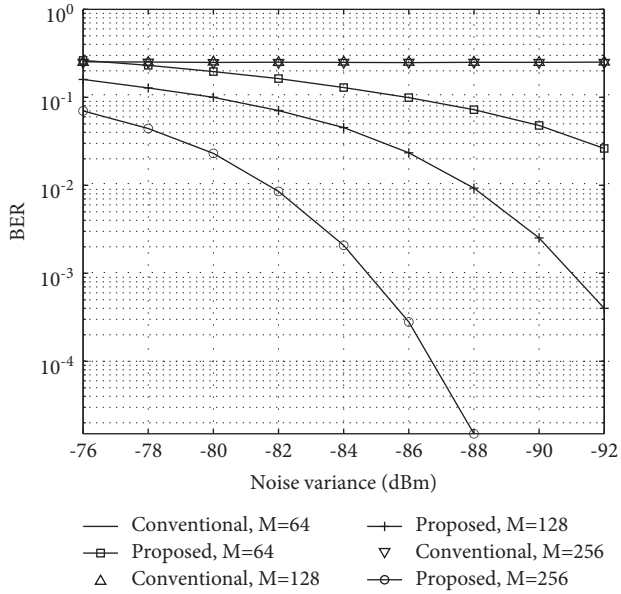

Figure 3: BER comparison for different sizes of RIS surface.

$$\hat{x}_{\mathrm{B}}(n) = \frac{z(n)}{\sqrt{P_{\mathrm{B}}}h_{\mathrm{B}}}. \tag{12}$$

4. Simulation Results

Several computer simulations are carried out in this section to evaluate the performance of the proposed method. QPSK modulation is adopted by two users who share the same time-frequency resources for transmission, as shown in (4). The channel is assumed to be a quasistatic fading channel, i.e., the channel remains constant within the block duration time, and changes to new independent realizations for the next block duration time. In simulation, we set $\rho_0 = -30$dB, , $d_0 = 50$m, , $\alpha_{\mathrm{RU}} = \alpha_{\mathrm{AR}} = 2.2$, and $K_1 = K_2 = 10$,, which are almost the typical values used in much of the literature that studies STAR-RIS [4–18]. Moreover, ideal channel estimation is assumed and no channel coding is considered.

Since we focus on the cell edge case, both users are assumed to have almost the same transmit power and distance to STAR-RIS. In current cellular systems, such as 5G UDN, a microcell usually has a radius of about 100 m [20]. So, we set $P_{\mathrm{A}} = P_{\mathrm{B}} = 30$dBm and $d_{\mathrm{A}} = d_{\mathrm{B}} = 50$m in simulation. Figure 3 shows BER performance comparison as a function of noise variance σ_n^2 for different sizes of STAR-RIS surface. For comparison, the conventional method where no element selection is performed is also simulated. As can be seen from Figure 3, if all the elements are activated to reflect the signal in the cell edge case, SIC cannot work. On the contrary, by selecting appropriate elements to activate, the BER curve can go down as the noise variance decreases. The BER comparison as a function of M is plotted in Figure 4 where the noise variance is fixed at −85dBm. From Figure 4, we can see that as M increases, the BER performance gain of the proposed method becomes larger. This is because more selected elements increase the strength of both users' signals at AP.

In Figure 5, we fix the transmit power of both cell edge users at 30dBm and vary the distance to compare their BER performance. In the simulation, we assume that $d_{\mathrm{A}} = 45$m, and $d_{\mathrm{B}} = 50$m, . From Figure 5, we find that when there is a sufficient distance difference between users, the conventional method can also work. However, the proposed method can enlarge this difference, and then achieve a better BER performance. Figure 6 compares the BER performances for different transmit powers where the distances of both cell edge users to STAR-RIS are kept at 50 m. In the simulation, P_{A} is set to 29dBm which is smaller than P_{B} of 30dBm. In this case, SIC can start to work. Similarly, as can be seen from Figure 6, the proposed method can still perform better than that of the conventional method.

Recently, an element splitting method has been proposed for RIS-aided NOMA uplink, in which a group of the surface reflecting elements is configured to boost the signal of one of the users, while the remaining elements are used to boost the other user [21]. The analysis shows that for small pathloss differences, the split should be chosen such that most of the elements are configured to boost the stronger user, while for large pathloss differences, it is more beneficial to boost the weaker user. Although the element splitting method is designed for conventional reflecting or transmitting RIS, it can also be used in STAR-RIS after some modifications. Figure 7 shows the BER performance comparison for the case of $M = 128$, $P_{\mathrm{A}} = P_{\mathrm{B}} = 30$dBm, and $d_{\mathrm{A}} = d_{\mathrm{B}} = 50$m. In the simulation, we assume that about 80% of the elements are used to transmit the signal of user A, and the left elements are set for reflecting user B's signal. When an element is chosen for transmitting, its total energy is allocated to the transmission coefficient and no energy is left for the reflection coefficient. In this case, $\beta_{\mathrm{A}} = 1$, $\beta_{\mathrm{B}} = 0$, and

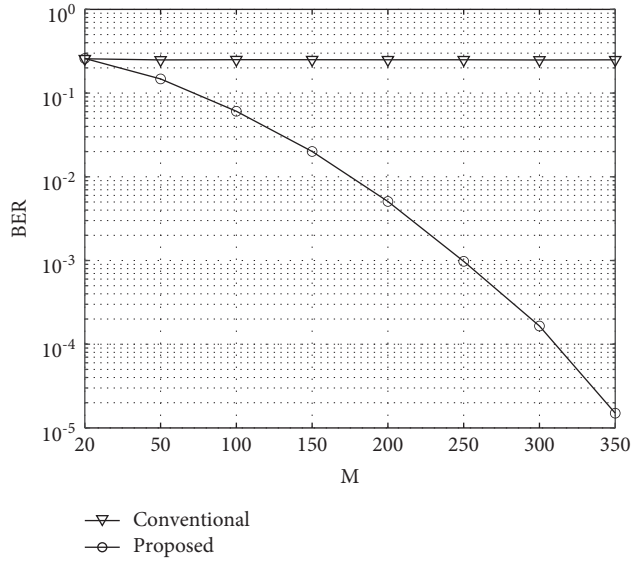

Figure 4: BER comparison as a function of M.

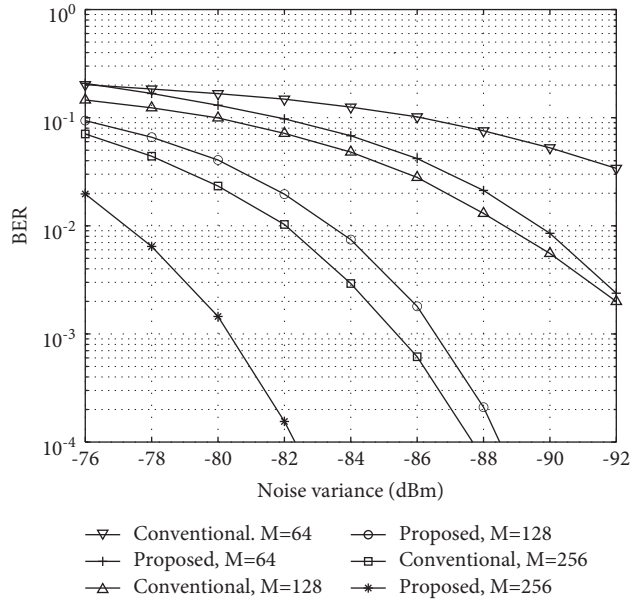

Figure 5: BER comparison for different distances.

$\theta_n^{\mathrm{A}} = \angle(F_{\mathrm{A}}(n) \cdot G(n))$. The same coefficient setting is applied for the element chosen for reflection, that is $\beta_{\mathrm{A}} = 0$, $\beta_{\mathrm{B}} = 1$, and $\theta_m^{\mathrm{B}} = -\angle(F_{\mathrm{B}}(m) \cdot G(m))$. From Figure 7, we find that the modified element splitting method performs better than the proposed method. This is because some elements are inactive in proposed method, which reduces the total channel gain at the receiver. In order to avoid this energy loss, we propose an enhanced element selection method where all the elements are active. When an element satisfies $\mu_{\mathrm{A}}(m) > \mu_{\mathrm{B}}(m)$,, all energy is allocated

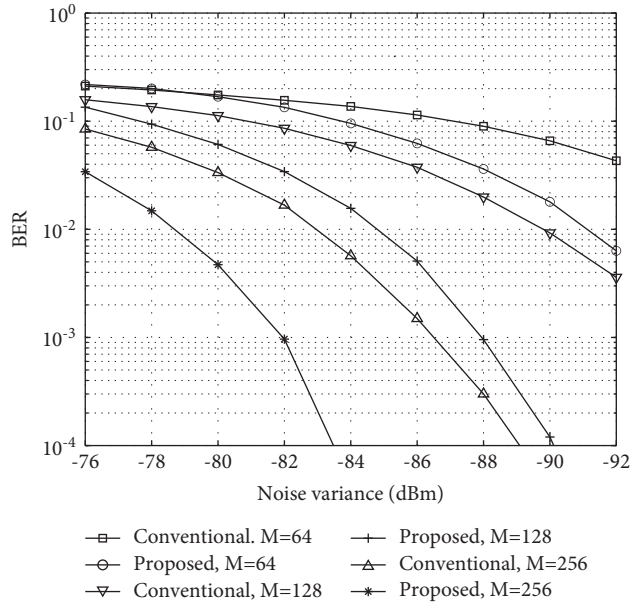

Figure 6: BER comparison for different transmit powers.

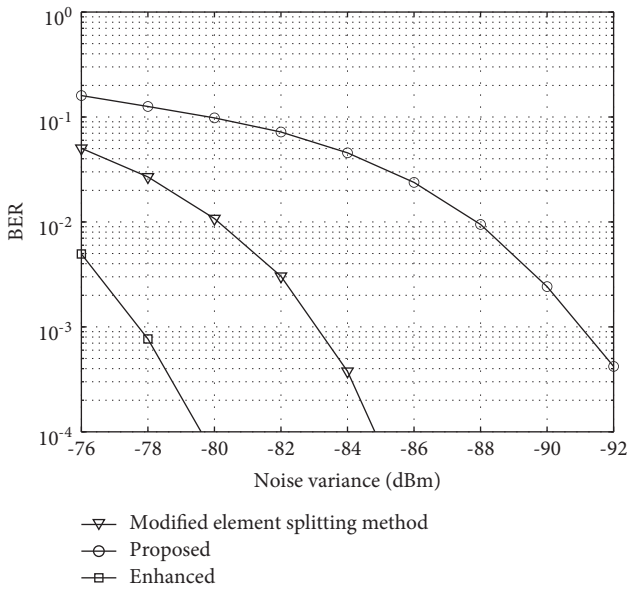

Figure 7: BER comparison for different methods.

to user A. i. e., $\beta_A = 1$, and $\beta_B = 0$. In the other case, total energy is divided equally between transmission and reflection coefficients. As can be seen from Figure 7, this method can achieve the best performance among all the methods.

5. Conclusions

In this paper, we focus on the cell edge users and propose a novel element selection method for STAR-RIS aided NOMA systems. In the proposed method, the individual channel paths reconfigured by each element in STAR-RIS for different users are compared and only the elements that can strengthen the channel of the desired user are selected to be activated. As a result, the whole cascade channel is reshaped into a favorable propagation environment for NOMA transmission. Simulation results show that a superior BER performance can be achieved at the receiver due to the better performance of SIC.

Data Availability

The data that support the findings of this study are available from the corresponding author upon reasonable request.

Conflicts of Interest

The authors declare that they have no conflicts of interest.

Acknowledgments

This work is supported by the National Key R&D Program of China (2020YFB1806603) and the Research and Development Center China, Sony (China) Ltd.

References

[1] Z. Ding, Y. Liu, J. Choi et al., "Application of non-orthogonal multiple access in LTE and 5G networks," *IEEE Communications Magazine*, vol. 55, no. 2, pp. 185–191, Feb. 2017.

[2] T. N. Do, D. B. da Costa, T. Q. Duong, and B. An, "Improving the performance of cell-edge users in NOMA systems using cooperative relaying," *IEEE Transactions on Communications*, vol. 66, no. 5, pp. 1883–1901, May 2018.

[3] S. Timotheou and I. Krikidis, "Fairness for non-orthogonal multiple access in 5G systems," *IEEE Signal Processing Letters*, vol. 22, no. 10, pp. 1647–1651, Oct. 2015.

[4] G. Yang, X. Xu, Y. C. Liang, and M. D. Renzo, "Reconfigurable intelligent surface-assisted non-Orthogonal multiple access," *IEEE Transactions on Wireless Communications*, vol. 20, no. 5, pp. 3137–3151, May 2021.

[5] F. Boccardi, R. W. Heath, A. Lozano, T. L. Marzetta, and P. Popovski, "Five disruptive technology directions for 5G," *IEEE Communications Magazine*, vol. 52, no. 2, pp. 74–80, Feb. 2014.

[6] Q. Wu, G. Y. Li, W. Chen, D. W. K. Ng, and R. Schober, "An overview of sustainable green 5G networks," *IEEE Wireless Communications*, vol. 24, no. 4, pp. 72–80, Aug. 2017.

[7] Q. Wu and R. Zhang, "Intelligent reflecting surface enhanced wireless network: joint active and passive beamforming design," *Proc. IEEE GLOBECOM*, pp. 1–6, Dec. 2018.

[8] Q. Wu and R. Zhang, "Towards smart and reconfigurable environment: intelligent reflecting surface aided wireless network," *IEEE Communications Magazine*, vol. 58, no. 1, pp. 106–112, Jan. 2020.

[9] T. J. Cui et al., "Coding metamaterials, digital metamaterials and programmable metamaterials," *Light: Science & Applications*, vol. 3, p. 218, Oct. 2014.

[10] C. Liaskos, S. Nie, A. Tsioliaridou, A. Pitsillides, S. Ioannidis, and I. Akyildiz, "A new wireless communication paradigm through software-controlled metasurfaces," *IEEE Communications Magazine*, vol. 56, no. 9, pp. 162–169, Sept. 2018.

[11] S. Bi, C. K. Ho, and R. Zhang, "Wireless powered communication: opportunities and challenges," *IEEE Communications Magazine*, vol. 53, no. 4, pp. 117–125, Apr. 2015.

[12] B. Zheng, C. You, and R. Zhang, "Fast channel estimation for IRS-assisted OFDM," *IEEE Wireless Communications Letters*, vol. 10, no. 3, pp. 580–584, Mar. 2021.

[13] Z. Ding and P. Vincent, "A simple design of IRS-NOMA transmission," *IEEE Communications Letters*, vol. 24, no. 5, pp. 1119–1123, May 2021.

[14] B. Tahir, S. Schwarz, and M. Rupp, "Analysis of uplink IRS-assisted NOMA under Nakagami-m fading via moments matching," *IEEE Wireless Communications Letters*, vol. 10, no. 3, pp. 624–628, Mar. 2021.

[15] M. Fu, Y. You, and Y. Shi, H. I. Waikola, Intelligent reflecting surface for downlink non-orthogongal multiple access networks," in *Proc. IEEE GLOBECOM Workshops,* pp. 1–6, USA, Dec. 2019.

[16] J. Xu, Y. Liu, X. Mu, and O. A. Dobre, "STAR-RISs: simultaneous transmitting and reflecting reconfigurable intelligent surfaces," *IEEE Communications Letters*, vol. 25, no. 9, pp. 3134–3138, May 2021.

[17] NTT, "DOCOMO conducts world's first successful trial of transparent dynamic metasurface," 2020, https://www.nttdocomo.co.jp/english/info/mediacenter/pr/2020/011700.html.

[18] C. Wu, Y. Liu, X. Mu, X. Gu, and O. A. Dobre, "Coverage characterization of STAR-RIS networks: NOMA and OMA," *IEEE Communications Letters*, vol. 25, no. 9, pp. 3036–3040, Sept. 2021.

[19] B. Sheng, "Optimal power allocation in STAR-RIS for CoMP transmission," *IEICE Communications Express*, vol. 11, no. 2, pp. 86–92, 2022.

[20] S. Adeshina, S. Mumtaz, S. Ai-Ruaye, and J. Rodriguez, "5G millimeter-wave mobile broadband: performance and challenges," *IEEE Communications Magazine*, vol. 56, no. 6, pp. 137–143, Jun. 2018.

[21] B. Tahir, S. Schwarz, and M. Rupp, "Outage analysis of uplink IRSassisted NOMA under elements splitting," in *Proceedings of the/IEEE Vehicular Technology Conference*, pp. 1–6, Helsinki, Finland, Apr. 2021.